Journal of Theoretical and Applied Mechanics, Sofia, 2013, vol. 43, No. 2, pp. 83–94

SIMULATION OF FLUID FLOW IN CENTRIFUGAL TRICANTER*

Cristian Puscasu, Mihaela Grigorescu, Axene Ghita, Raluca Voicu, Mariana Stefanescu, Victoria Teleaba
National Research & Development Institute for Gas Turbines COMOTI,
I220D, Iuliu Maniu Avenue, sector 6,
Code 061126, OP76, CP 174, Bucharest, Romania,
e-mail: cristian.puscasu@comoti.ro

Ivanka Zheleva,
Ruse University "Angel Kanichev",
8, Studentska Street, 7017, Russe, Bulgaria,
e-mail: izheleva@uni-ruse.bg

[Received 19 November 2012. Accepted 03 June 2013]

Abstract. An ANSYS simulation of the multiphase complex fluid flow motion in a centrifugal device (tricanter) is presented in the paper. This centrifugal device is designed for one step efficient solution for contaminated river water processing with oil and oil products. The proposed tricanter is one of the main objectives of the project named "Common strategy to prevent the Danube's pollution technological risks with oil and oil products CLEANDANUBE" financed by European Commission within the frame of Romania-Bulgaria Trans-Border Cooperation Program 2007 – 2013 (grant MIS-ETC code 653). Results for liquid phases (water and oil products) and for solid particles motion are presented graphically and are commented.
Key words: Complex multiphase flow simulation, centrifugal device (tricanter).

1. Introduction

This study is a part of scientific work of the project named "Common strategy to prevent the Danube's pollution technological risks with oil and oil products CLEANDANUBE" financed by European Commission in the frame of Ro-Bg Trans-Border Cooperation Program 2007 – 2013 under grand MIS-ETC code 653.

*Corresponding author e-mail: izheleva@uni-ruse.bg

Lead partner of the project is National Research & Development Institute for Gas Turbines COMOTI, Bucharest, Romania and Partner 2 of the project is Ruse University "Angel Kanchev".

The executive team is:

- from COMOTI Institute – Puscasu Cristian, Stefanescu Mariana, Voicu Raluca, Axene Ghita, Grigorescu Mihaela, Adam Liviu, Cretu Mihaela, Precob Luminita, Toma Emilian, Teleaba Victoria, Antonescu Marilena;
- from Ruse University – Ivanka Mitkova Zheleva, Gencho Popov, Piter Russev, Peter Kopchev, Krasimir Tuzharov, Kliment Klimentov, Ivaylo Nikolaev, Yana Kraleva.

Project manager is d-r Cristian Puscasu from COMOTI Institute and project coordinator of the second partner Ruse University is assoc. prof. Ivanka Zheleva.

The main project objectives are:

- Romanian – Bulgarian common strategy for accidents and technological risks pollution management of the Danube water with oil products;
- One step efficient solution for centrifugal processing of contaminated water with oil products in order to reduce pollution risks.

In this study we present a simulation of the fluid flow motion in the centrifugal device for one step processing of the contaminated with oil products water.

2. Statement of the problem

For this study, the flow was assumed compressible, the equations that govern the flow, written in Reynolds averaged form, time and mass averaged [1, 2, 3], being, in the repeated indices summation convention:

The Continuity Equation:

$$\frac{\partial \overline{\rho}}{\partial t} + \frac{\partial \overline{\rho}\tilde{u}_j}{\partial x_j} = 0. \tag{1}$$

The Momentum Equations:

$$\frac{\partial \overline{\rho}\tilde{u}_i}{\partial t} + \frac{\partial \overline{\rho}(\tilde{u}_i\tilde{u}_j)}{\partial x_j} = -\frac{\partial \overline{p}}{\partial x_i} + \frac{\partial}{\partial x_j}\left(\overline{\tau_{ij}} - \overline{\rho u_i' u_j'}\right), \tag{2}$$

where

$$\overline{\tau_{ij}} = \mu\left[\frac{\partial \tilde{u}_i}{\partial x_j} + \frac{\partial \tilde{u}_j}{\partial x_i} - \frac{2}{3}\delta_{ij}\left(\frac{\partial \tilde{u}_k}{\partial x_k}\right)\right]$$

represents the stress tensor.

The Total Energy Equation:

$$\frac{\partial}{\partial t}\left(\bar{\rho}\tilde{h}\right)+\frac{\partial\left(\overline{\rho}\tilde{u}_j\tilde{h}\right)}{\partial x_j}=\frac{\partial\overline{p}}{\partial t}+\frac{\partial}{\partial x_j}\left(\overline{\frac{\mu}{\mathrm{Pr}}\frac{\partial h}{\partial x_j}}\right)+\frac{\partial}{\partial x_j}\left(-\overline{\rho h'u_j'}\right), \tag{3}$$

where h is the enthalpy.

Ideal Gas Equation of State:

$$\tilde{\rho}=\frac{w\left(\tilde{p}+p_{ref}\right)}{R_0\tilde{T}}, \tag{4}$$

where w is the molecular weight

The k-ε two-equation turbulence model is employed in order to close the correlation type terms which appear in the above equations. The model uses the gradient diffusion hypothesis to relate the Reynolds stresses to the mean velocity gradients and the turbulent viscosity. The turbulent viscosity is modelled as the product of a turbulent velocity and turbulent length scale.

In the two-equation class models, the turbulence velocity scale is computed from the turbulent kinetic energy, which is provided by numerically solving its transport equation along with the governing equations presented earlier. The turbulent length scale is estimated from two properties of the turbulence field, in this case the turbulent kinetic energy, k, and its dissipation rate, ε. The dissipation rate of the turbulent kinetic energy is also provided by numerically solving its transport equation.

$$\frac{\partial\left(\rho k\right)}{\partial t}+\nabla\left(\rho U k\right)=\nabla\left[\left(\mu+\frac{\mu_t}{\sigma_k}\right)\nabla k\right]+P_k-\rho\varepsilon. \tag{5}$$

$$\frac{\partial\left(\rho\varepsilon\right)}{\partial t}+\nabla\left(\rho U\varepsilon\right)=\nabla\left[\left(\mu+\frac{\mu_t}{\sigma_\varepsilon}\right)\nabla\varepsilon\right]+\frac{\varepsilon}{k}\left(C_{S_1}P_k-C_{S_2}\rho\varepsilon\right). \tag{6}$$

Where C_{S_1} , C_{S_2}, σ_k, σ_ε are model constants, and P_k is the turbulence production due to viscous forces which are modelled using the following formula [3]:

$$P_k=\mu_t\nabla U\left(\nabla U+\nabla U^T\right)-\frac{2}{3}\nabla U\left(3\mu_t\nabla U+\rho k\right) \tag{7}$$

These equations are discretized using a second order upwind scheme.

3. Setup and boundary conditions of the numerical simulations

Aerodynamic computational model implies certain modifications from the real model. Basically, what is kept is the path of the working fluid inside our tricanter centrifuge (Fig. 1):

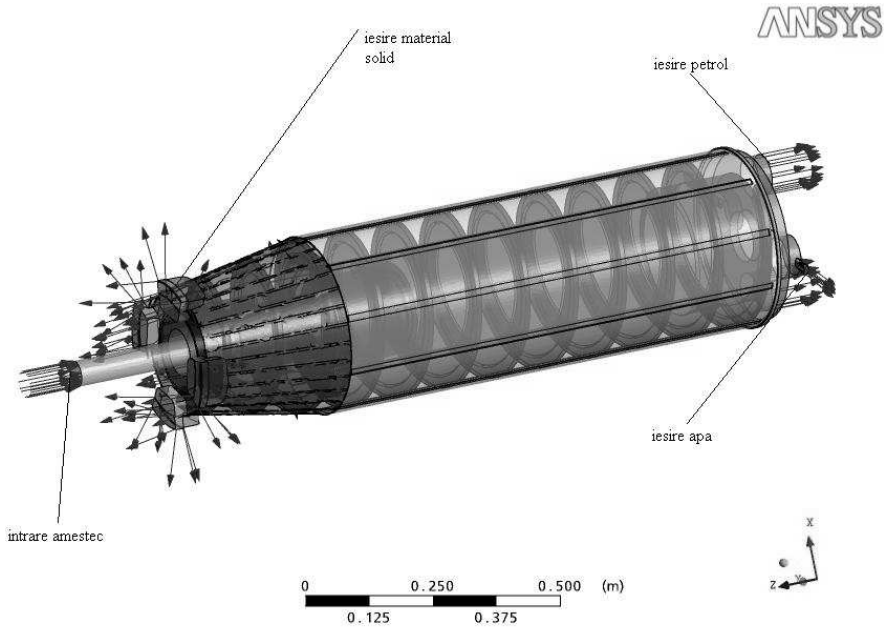

Fig. 1. Computational domain

Initial conditions are the following: Mass flow: 20 m^3/h, Inlet: – mixture: water + oil in liquid form; Water density: 1000 kg/m^3, Oil density: 800 kg/m^3, Temperature : 293 K, Total pressure: 5 bar, Turbulence intensity: 5 %, Oil volume fraction: 0.7116, Water volume fraction: 0.2884, Solid particles: Density: 2011 kg/m^3, Inlet speed: 10 m/s, Mass flow: 68 g/s, Particle minimum diameter: 20 de microns, Particle maximum diameter: 60 de microns, Outlet: Mass flow: 20 m^3/h, Casing: Speed: 4000 rot/min, Centrifugal rotor: Speed: 3960 rot/min, The solid walls were considered adiabatic (no heat transfer), impermeable and no-slip (zero velocity at the wall).

For this case, an unstructured grid had been used because the complexity of the tricanter makes the problem too computationally expensive for a structured grid. Also, local refinements have been used in order to be able to control the total number of cells. We use ANSYS CFD software package for simulation of this very complicated fluid motion in the centrifugal tricanter [5].

4. Results

In the following, we present the results of the aerodynamic analysis of the tricanter centrifuge.

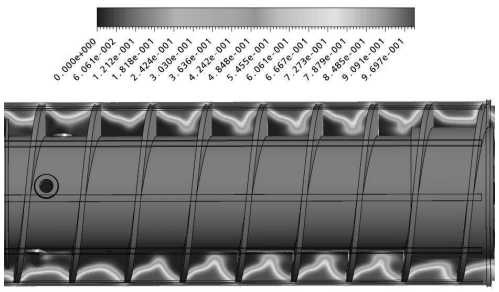

Fig. 2. Water volume fraction around the centrifugal rotor

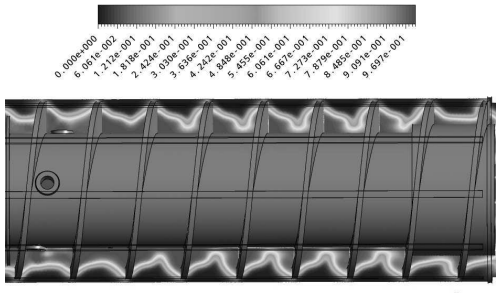

Fig. 3. Oil volume fraction around the centrifugal rotor

As one can see, in Fig. 2 the biggest water concentration is near the casing, and this is due to higher water density than the density of oil. Also, the water concentration is zero or almost zero close to centrifugal rotor body.

It is possible to see in Fig. 3, that oil concentration is almost zero or zero exactly where the water concentration is the biggest (Fig. 2). This shows that the separation of the mixture starts around the centrifugal rotor.

The irregularity of the flow due to complex geometry can be observed in Fig. 4. Also it can be seen, that the mixture separation starts before entering

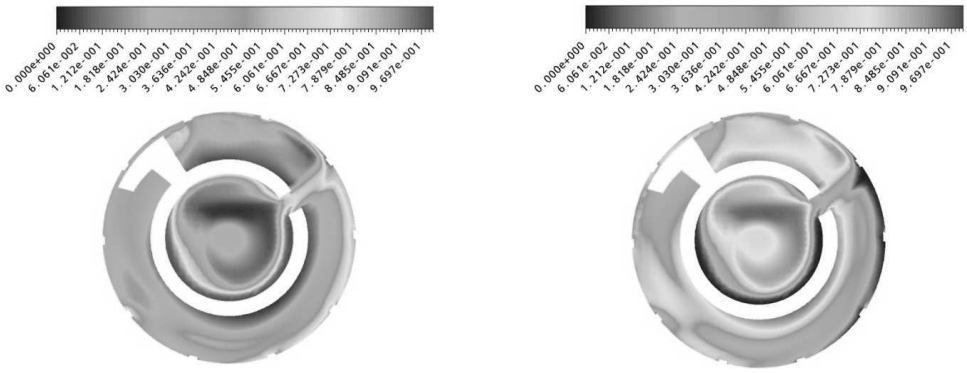

Fig. 4. Water (a) and oil (b) volume fraction at the first entrance in the centrifugal rotor

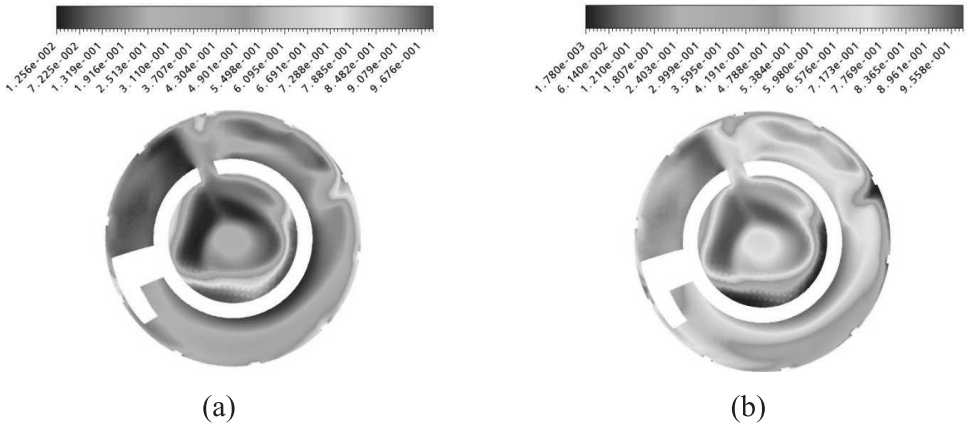

Fig. 5. Water (a) and oil (b) volume fraction at the second entrance in the centrifugal rotor

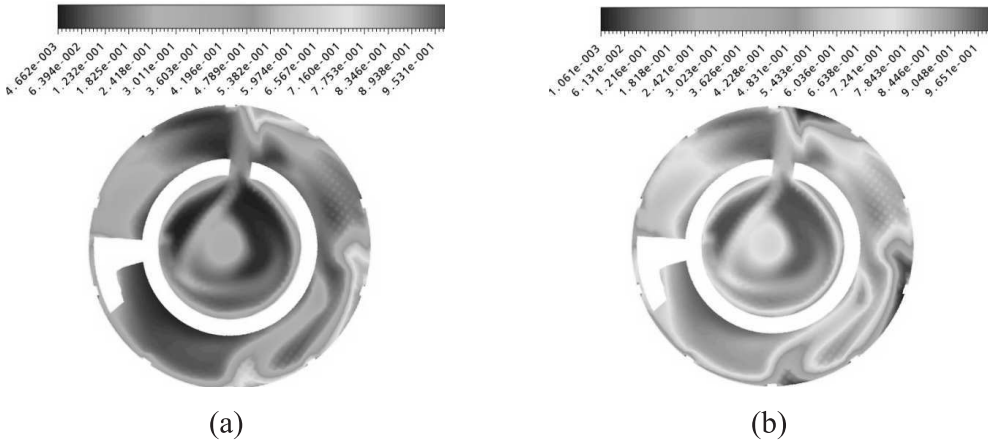

Fig. 6. Water (a) and oil (b) volume fraction at the third entrance in the centrifugal rotor

the centrifugal rotor, as it can be observed the water is concentrated on the walls and the oil in the middle.

Also, in Fig. 5 we can see the same characteristic of the flow.

In Figs 4–7 it can be observed how the water concentration is decreasing as the mixture approaches the fourth entrance. A possible explanation is that the water enters the centrifugal rotor faster then the oil through the first entrances.

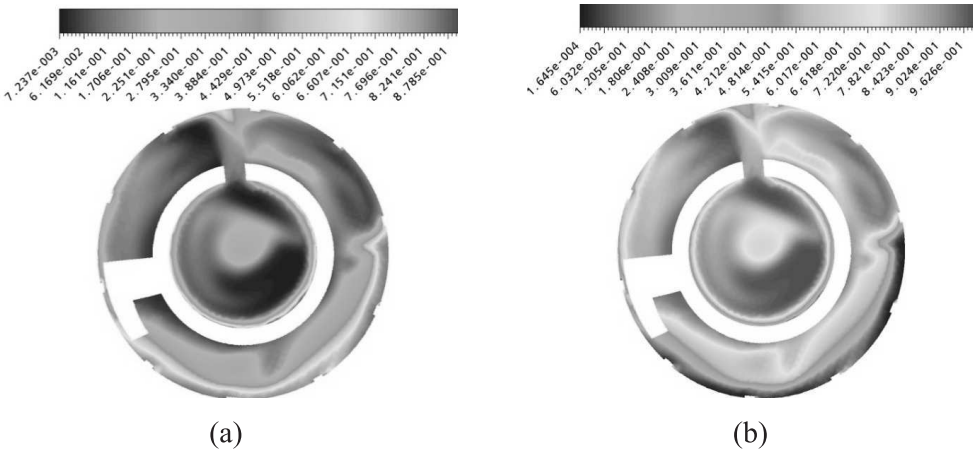

Fig. 7. Water (a) and oil (b) volume fraction at the fourth entrance in the centrifugal rotor

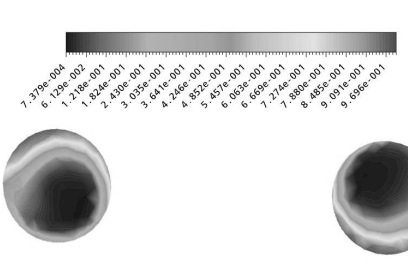

Fig. 8. Water volume fraction at oil outlet

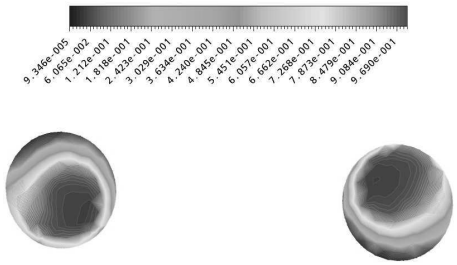

Fig. 9. Oil volume fraction at oil outlet

In Figs 8 and 9 it can be observed that on the oil outlet the dominant fluid that exit through this outlet is oil.

In Figs 10 and 11 it can be observed that on the water outlet exit only water. In Fig. 13 it can be seen that the water and oil concentration is low due to the fact that solid particles partially blocks the flow channel. We have to observe first the vector field, Fig. 13, in order to understand how these solid particles behave. Here, it can be observed the recirculation zones that are produced before entering the centrifugal rotor and also inside the centrifugal rotor. The recirculation zones affect not only the flow but also the solid particles behaviour.

In Fig. 14, it can be observed where the highest concentration of particles at the four entrances is. This evolution shows that the particles are caught

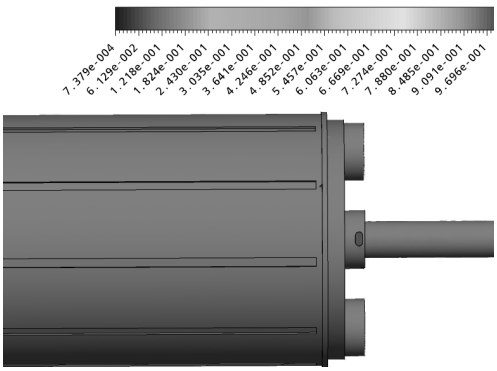

Fig. 10. Water volume fraction at water outlet

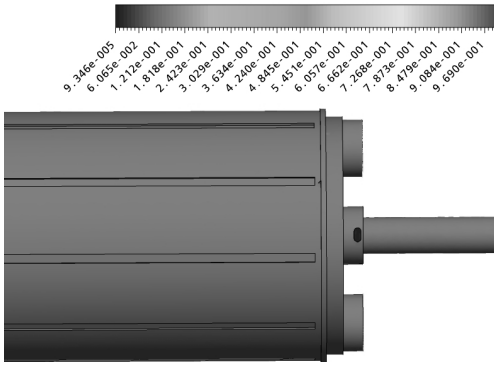

Fig. 11. Oil volume fraction at water outlet

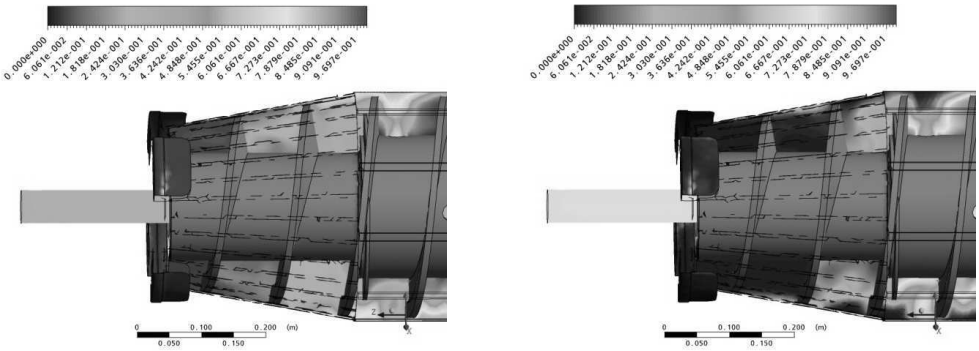

(a) (b)

Fig. 12. Water (a) and oil (b) volume fraction in frontal part of the trincanter centrifuge

inside the tricanter centrifuge between the recirculation zones.

Particles evolution is correct because the flow has an inverse sense of rotation than the casing and centrifugal rotor (Fig.13). So, the flow directs the particles that passes through the space between centrifugal rotor and casing (Fig. 14) towards the outlet situated in the frontal part of the tricanter centrifuge.

5. Conclusion

1. The inside tricanter centrifuge flow analysis is performed. During this analysis, the influence of oil is considered, water and solid particles, also.

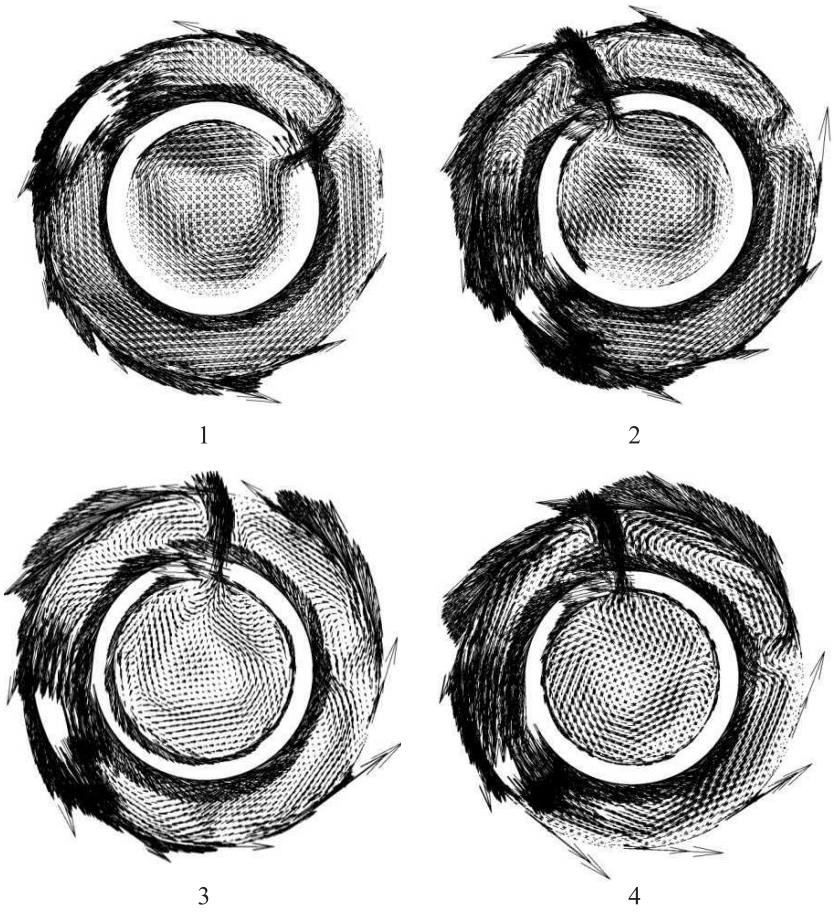

Fig. 13. Vector field at the entrances inside the centrifugal rotor

2. Inside the tricanter centrifuge the separation of water, oil and solid parts are performed efficiently.
3. At the outlet it is possible to see, that on the water outlet comes out water, on the oil outlet comes out oil and on the solid particles outlet come out solid particles, mainly.
4. In the next stages, is proposed to run the simulation program with other initial conditions both functional and technological.

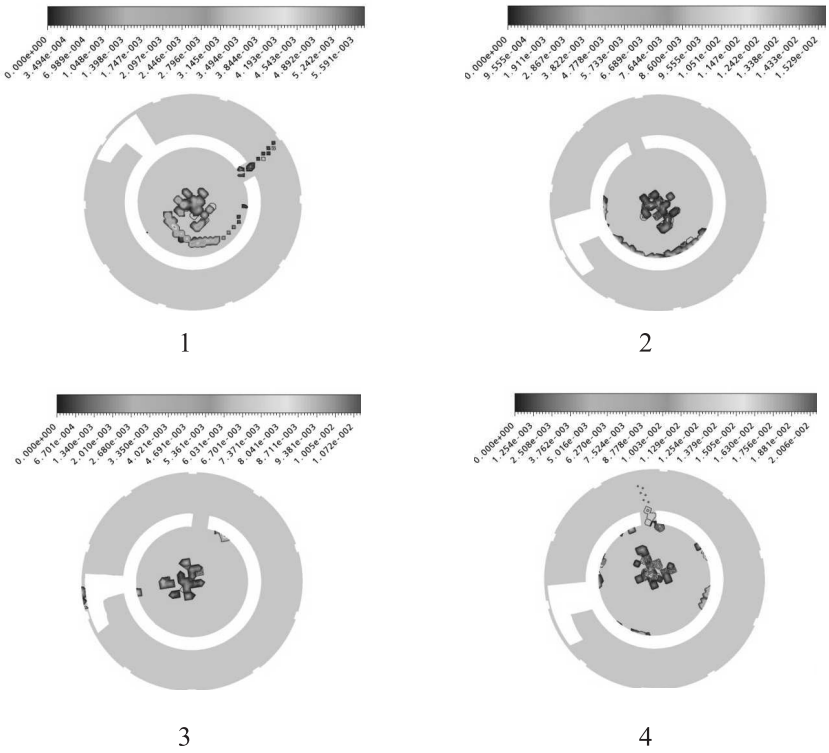

Fig. 14. Volume fraction of the solid particles in the domain

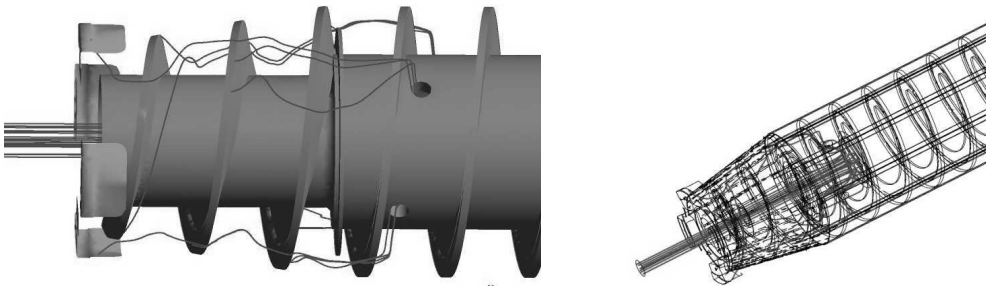

Fig. 15. Solid particles behaviour in the domain

Nomenclature

D_I	kinematic diffusivity [m^2/s]	R	universal gas constant [J/kgK]
t	time [s]	p	pressure [N/m^2]
h	specific thermodynamic enthalpy [J/kg]	S_I	is the source term due to chemical reaction rate involving component I
R_K	elementary reaction rate of progress for reaction $\boldsymbol{k}$	P_k	turbulence production due to viscous forces
k	specific turbulent kinetic energy per unit mass [m^2/s^2]	T	temperature [K]
W_I	molar mass [kg/kmol]	C_{S1}	model constant [–]
w	molecular weight [kg/kmol]	u	velocity [m/s]
Y	mass fraction [–]	C_{S2}	model constant [–]

Greek characters

δ	Kronecker delta [–]	μ	dynamic viscosity [kg/(ms)]
ρ	density [kg/m^3]	τ_{ij}	turbulent stress tensor [m^2/s^2]
ε	dissipation rate of the turbulent kinetic energy per unit mass [m^2/s^3]	ν	kinematic viscosity [m^2/s]
ν_{kI}	stoichiometric coefficient for component	σ_k	model constant [–]
σ_ε	model constant [–]	Γ_i	diffusion coefficient of component I [m^2/s]

Dimensionless number Pr – Prandtl number

Statistical quantities

$\overline{\phi}$ – time or ensemble average of variable ϕ
ϕ' – fluctuating part of variable ϕ
$\tilde{\phi}$ – filtered variable ϕ

REFERENCES

[1] Tannehill, J. C., D. A. Anderson, R. H. Pletcher. Computational Fluid Mechanics and Heat transfer, ISBN 1-56032-046-X, Taylor & Francis, 1997-04-01 Hardcover, 816 pp.

[2] Lesieur, M. Turbulence in Fluids, 3rd edition, Kluwer Academic Publishers, 1997, 288 pp., ISBN 0-7923-4415-4(HB).

[3] CFM International CFM56, www.janes.com

[4] ICAO Engine Exhaust Emissions Data Bank, https://cwcs.cfm56.com/CWCTour/CWC_ONLINE/image/image\%20divers/CFM56-7B27-2.pdf

[5] ANSYS Software Package ANSYS Resources http://www.caeai.com/all-downloads.php